

# Magnetic treatment of industrial water. Silica activation

A. Szkatuła, M. Bałanda<sup>a</sup>, and M. Kopeć

H. Niewodniczański Institute of Nuclear Physics, Radzikowskiego 152, 31-342 Kraków, Poland

Received: 24 April 2001 / Received in final form: 18 October 2001 / Accepted: 13 December 2001

**Abstract.** The paper presents two large-scale observations of magnetic treatment of industrial water, aimed at investigating changes in the formation of deposits. First, a four-month experiment is described with two identical 25 kW heat exchangers, where in one case the inlet water was treated by a magneto-hydrodynamic method. Deposits recovered from both exchangers were analyzed chemically, by X-ray diffraction, infrared spectroscopy and PIXE. The amount of deposit for untreated water, composed mostly of calcite, increased exponentially with temperature reaching 20 g/m of tube at the warm end of the heat exchanger. The mass of the deposit for magnetically treated water did not depend on temperature and was only *ca.* 0.5 g/m of tube. It was composed of mainly noncrystalline silica-rich material. Further results were obtained from the practical installation at three blocks of a 1 GW power plant. The soft, amorphous deposit for magnetically treated water had a specific surface area of 80 m<sup>2</sup>/g and an infrared spectrum similar to that of a silicate hydrogel. Therefore, it appeared that, as a result of the passage through the magnetic device, crystallization of carbonates in water was blocked due to initiation of another, competitive process. This process is the activation of the colloidal silica, which will adsorb calcium, magnesium or other metal ions and then precipitate from the solution as the coagulated agglomerate. The most probable mechanism responsible for silica activation is a Lorentz-force induced deformation of the diffuse layer leading to the increased counterion concentration in the adsorption layer of the negatively charged silica.

**PACS.** 85.70.-w Magnetic devices – 82.70.Dd Colloids – 33.20.Ea Infrared spectra

## 1 Introduction

Influence of magnetic field on phenomena occurring in aqueous solutions, or other nonmagnetic systems, have been an interesting subject. The problem, which is still not well understood, is a reduction of formation a limescale from hard water on pipelines surfaces by the magnetic water treatment (MWT). It is known that the build up of scale deposits is a common and costly problem in all processes where water is heated or used as a coolant. Since the patent of Vermeiren [1] various types of MWT devices are widespread involving usually a field of low flux density oriented perpendicularly to the water flow. In case of the proper MWT the following results can be obtained: formation of small amounts of slimy, easily washable deposits instead of the hard carbonate scale, slow dissolution and removal of old deposits, clarification of water containing suspended matter [2–6]. However, reported MWT effects are sometimes not consistent or not reproducible. This is probably due to variations in water composition, differences in the course of the treatment and to a complexity of processes, which occur in water solutions. It is puzzling that MWT is almost always effective in industry conditions. Another interesting problem is a positive influence of MWT on biological processes [7].

The early research carried out during 1960–1980, mainly in Russian institutes [2, 4, 5, 8, 9], did not supply a satisfying physico-chemical model which could account for all the observed phenomena. The idea of changes in structure of water itself, as a result of magnetic exposure has been criticized [8] due to the low field intensities used. For a long time, a simple qualitative inspection was used to describe changes taking place in water solutions and in deposits precipitated from water due to passage through a magnetic device. Very often, it was not even decided whether the slimy sediments were composed only of carbonates, or also of some other substances. The hypothesis was accepted that in magnetically treated water, crystallization of carbonates still occurs, yet not at the surface of boilers but throughout the whole volume of liquid. A test for efficiency of a method was usually the size of calcite grains: the smaller calcite grains formed in the conditioned water, the better the efficiency of treatment.

For several years one has observed growing efforts to find an explanation for the MWT effect. Since natural water presents a complex system in which besides hydrated ions, molecules and gas bubbles one deals with disperse colloidal particles of organic and inorganic compounds, it seemed plausible that explanation could be found in changes of ion distribution of the diffuse layers. The influence of MWT on the electrokinetic  $\zeta$ -potential of CaCO<sub>3</sub> suspension was measured already in [9]. The

---

<sup>a</sup> e-mail: maria.balanda@ifj.edu.pl

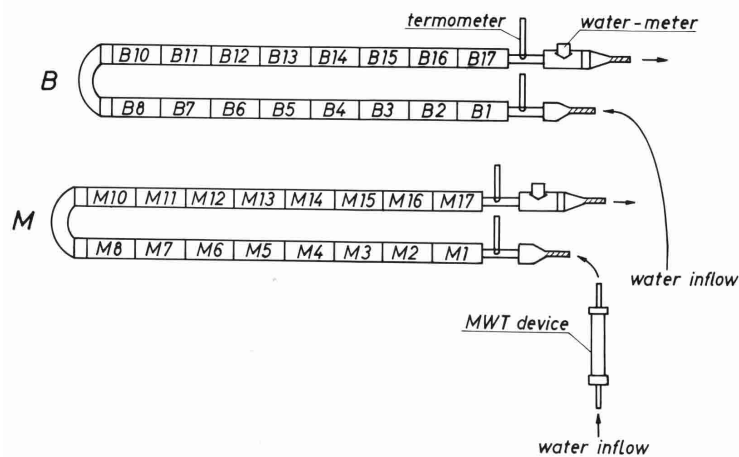


Fig. 1. Scheme of the experimental loops.

decrease of  $\zeta$ -potential was associated with an accelerated coagulation. Next, Higashitani *et al.* have conducted a series of well-controlled experiments of magnetic effects on static (not moving) aqueous solutions [10–13]. It was found in [10] that rapid coagulation rate of nonmagnetic colloidal particles depended on the magnetic flux density and the effect of a field grew up for smaller particle size. The decrease of  $\zeta$ -potential, which could be detected for at least 6 days was measured in [11]. In the paper [12] the authors used the atomic force microscope (AFM) to obtain the information of the magnetic effects on the molecular level. Thickness of the layer adsorbed on the surface in aqueous solutions changed after magnetic exposure, it was dependent on electrolyte concentration and showed a memory effect for at least a day. In the work [13] from 1999 the same group performed the AFM measurements in pulse and alternating magnetic fields and compared the results with that from the static field. It was found that the magnetic effect depended on the frequency of the pulse magnetic field and that the time required to reach the maximum effect was much smaller for the pulse and alternating fields than for the static field. Undoubtedly, the above AFM results present an important experimental evidence of phenomena responsible also for the antiscaling effect of MWT.

Analytical measurements dealing with the influence of magnetic fields on physical phenomena and chemical kinetics in water solutions have been reviewed by Barret and Parsons [14]. It appeared that results concerning pH, conductivity, particle size, turbidity and zeta potential were often inconsistent or even contradictory. Two likely MWT mechanisms were generally accepted: the action of microcontaminants and the Lorentz force induced effects on the solid-liquid interface. The later include changes in hydration shells around ions and in charge double layers. Another paper, based on blind laboratory tests, published by Coey and Cass [15] showed that effects of MWT carried out in a static magnetic field of 0.1 T persisted for more than two hundred hours.

It has been already mentioned that magnetic treatment of industrial waters is usually effective and helps

to reduce limescale formation. On the other hand, there is an understandable reluctance to make available any industrial installation for the purposes of scientific experiments with a proper control. We were fortunate in the period 1985–1990 to be able to set up a large-scale experiment at a power station in Poland. The first part of the paper describes that unique experiment. Water was flowing through the two identical loops simulating industry heat exchangers. In one case the inlet water was magnetically treated. The analysis of the deposits recovered from each loop after a four-month run showed remarkable changes caused by the magnetic treatment. The total mass of the deposit from the MWT loop was *ca.* 25-times less than the mass of the deposit from the non-treated water. The content of calcite in the deposit was lowered. Therefore, bigger, optimized magneto-hydrodynamic devices were constructed for the cooling system of the 1 GW power station. The efficiency of the treatment was excellent. Results of analyses of the deposits were consistent with those obtained in the large-scale experiment and allowed us to get better understanding of the essence of the MWT effect. The recent model of Lipus *et al.* [16], concerning surface neutralization due to ion shifts from the bulk of the solution toward the particle surfaces gives the good support for our conclusions.

## 2 Experimental methods

For the experiment, the two identical loops, B and M, simulating a heat exchanger of a power station, have been constructed. The loops were each made of 16 brass sections (tubes 1 m long,  $\Phi_{in} = 30$  mm, 1 mm wall thickness) and a bent piece, placed in the middle. The tubes were heated with an AC of 1.5 kW power used for each section. The MWT device was installed in front of one loop, designated the M-loop. A schematic diagram of the experiment is given in Figure 1. Figure 2a presents the scheme of the device. The apparatus was of cylindrical symmetry and used a stack of strontium ferrite permanent magnets placed in the ferromagnetic pipe. The cylindrically shaped

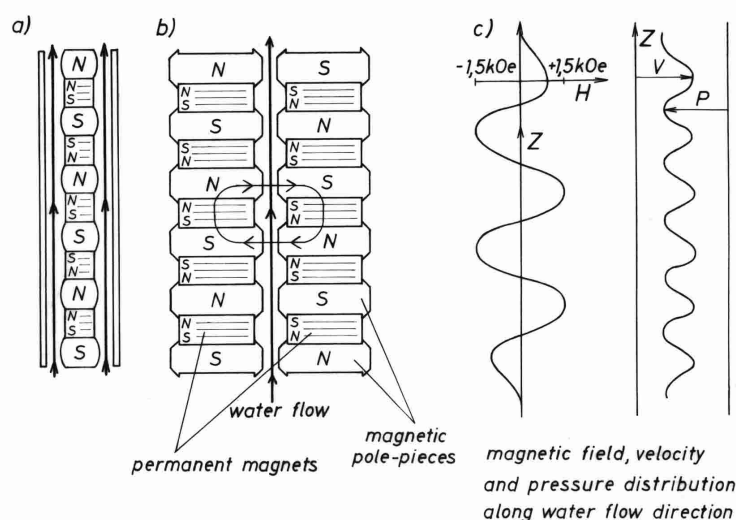


**Fig. 2.** Scheme of the MWT devices used: (a) large-scale experiment described in Chapter II; (b) industrial application described in Chapter IV; (c) magnetic field, pressure and velocity distribution along water-flow direction.

magnets of  $\Phi_{\text{out}} = 35$  mm,  $\Phi_{\text{inn}} = 5$  mm and the height equal to 15 mm, arranged with alternating polarity, were interspersed with magnetic steel pole-pieces. The rings were magnetized parallel to their axes. The pole-pieces had a diameter 4 mm greater than the magnets so there is a periodic water velocity change (from 1.0 to 1.6 m/s) in addition to the field profile. The field amplitude was 120 kA/m (1.5 kOe). The inner pressure of flowing water was also fluctuating, as shown in Figure 2c.

The inlet water was taken directly from a nearby lake. The results of chemical analysis, on average through the period of 4 months, were following: Ca–63 mg/l, Mg–27 mg/l, Fe–0.11 mg/l,  $\text{SO}_4^{2-}$ –37.0 mg/l (0.77 mval/l),  $\text{NO}_3^-$ –0.15 mg/l (0.002 mval/l),  $\text{Cl}^-$ –20.2 mg/l (0.57 mval/l), no free  $\text{CO}_2$ , pH = 8.3,  $\sigma = 67$  ms/m, total hardness–5.45 mval/l, carbonate hardness–5.2 mval/l, total suspended solids–14.7 mg/l,  $\text{SiO}_2$ –10 mg/l, total solid residue–356 mg/l. The water flow rate in each loop was 1.2 m<sup>3</sup>/h. The experiment was run in autumn and winter and lasted 4 months. During this time *ca.* 5000 m<sup>3</sup> flowed through it, and *ca.* 150 000 kWh was used to heat water.

The deposits recovered from both loops after the 4 months experiment were investigated by chemical analysis and by X-ray diffraction and PIXE (Proton Induced X-ray Emission) methods. Infrared absorption spectra were measured later.

### 3 Results

During the four-month run no significant difference could be detected in alkalinity, hardness and pH of water used in loop B (untreated water) and loop M (magnetically treated water). There was also no difference in the temperature profile or flow rate. Temperature increased linearly from 10 °C at the first section up to 30 °C at the last one. The inlet water temperature fell to 8 °C in winter.

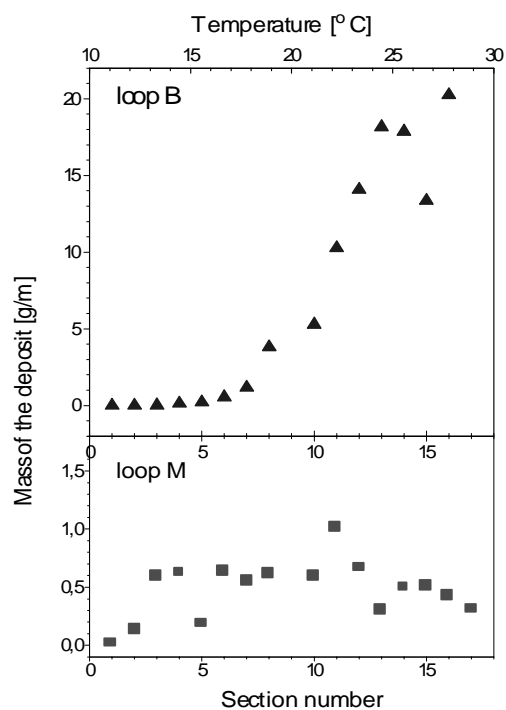


**Fig. 3.** Amount of the deposit, as a function of section number and/or temperature, recovered in loop B and loop M after a 4-months run.

The striking difference was in the quantity, the form and composition of the deposits recovered from two loops and also in the kinetics of precipitation of the sediment. The deposit from the tubes of loop B (the total mass of 190 g) was a hard scale, difficult to remove, while the one from the M loop (the total mass of 7 g) was soft and easy to remove. Amounts of deposit expressed in gram/meter of tube are given for the two loops in Figure 3. In loop B (see Fig. 3a) the amount of deposit increased

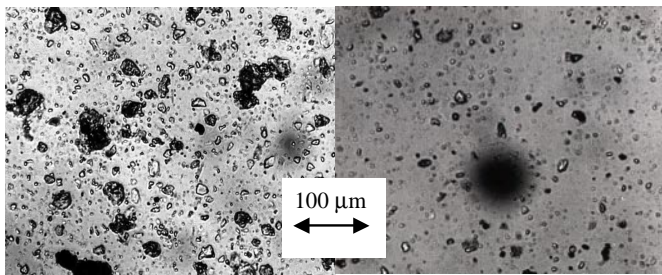


**Fig. 4.** Microscope pictures of the deposit from untreated water (left) and magnetically treated water (right).

exponentially with distance and temperature, starting from zero in the first three sections and reaching 20 g/m at the warm end. The activation energy inferred for the observed process is 15.11 kJ/mol. In contrast to case B, the mass of the deposit in loop M with magnetic treatment (see Fig. 3b) showed quite different dependence on temperature. An accelerated coagulation and sedimentation of suspended matter was observed already in first sections, as in the loop B at the same temperature there was no deposit at all. On the other hand the precipitation of sediment did not change with temperature and was constant at  $(0.5 \pm 0.2)$  g/m. Even at the warm end of the loop the mass of the deposit has not increased.

Figure 4 shows microscope pictures of deposits from untreated and magnetically treated water. One can notice that the B deposit consists of larger grains while the M deposit has smaller grains and more of the fine dispersed phase.

The chemical composition of the deposits, expressed in weight percentage, is given in Table 1. Large differences in the content of silica, potassium (as  $K_2O$ ), iron (as  $Fe_2O_3$ ), zinc (as  $ZnO$ ) and copper (as  $CuO$ ) can be seen. The amount of the above listed elements is several times higher for sections of the loop M than for appropriate sections (same numbers) of the loop B. On the other hand, the content of calcium (as  $CaO$ ) and magnesium (as  $MgO$ ) is lower for the loop M.

The analysis performed by PIXE for a pair of samples from B and M sections No. 15 (see Fig. 5) gives the same result: there is several times more of Cu, Zn, and Mn and over ten times more Fe for the deposit from the loop M.

The differences in the crystallochemical composition of the deposits are seen from the X-ray diffraction patterns (Fig. 6). The pattern of the deposit from the untreated water has a weak background due to the low contribution of the amorphous phase. Reflections are slightly shifted in comparison to those coming from pure calcite (see Fig. 6 in the middle). This points to rapid crystallization of Mg-substituted calcite (about 7% of Mg in the cation lattice, as determined from the lattice parameters). The background of the diffraction pattern for the deposit from the magnetically treated water is relatively high, so it comes from amorphous substances. The reflections correspond to  $\alpha$ -quartz and a small amount of pure calcite.

In order to explain the origin of the amorphous phase and to find the substance (or substances) of which it

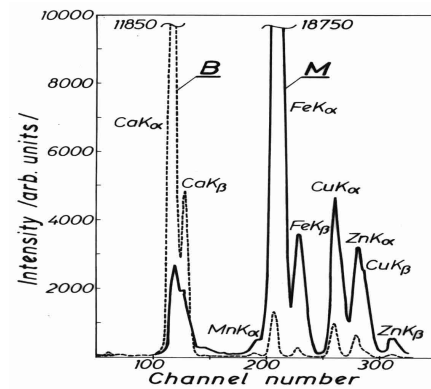


**Fig. 5.** Analysis of deposits performed by means of the PIXE method: full line - loop M (magnetic treatment), dotted line - loop B (no MWT).

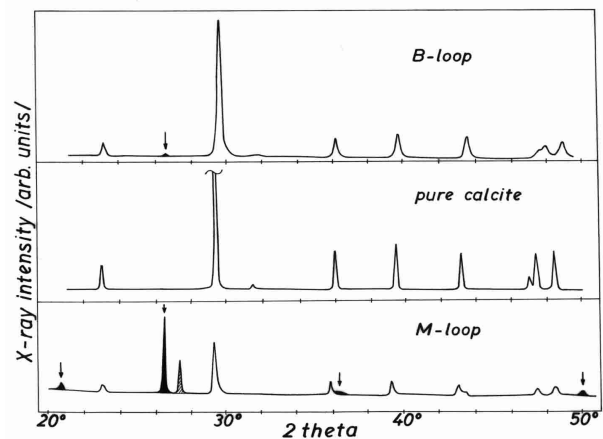


**Fig. 6.** X-ray diffraction patterns (Cu radiation) for deposits from both loops: the pattern of pure calcite is shown for comparison.

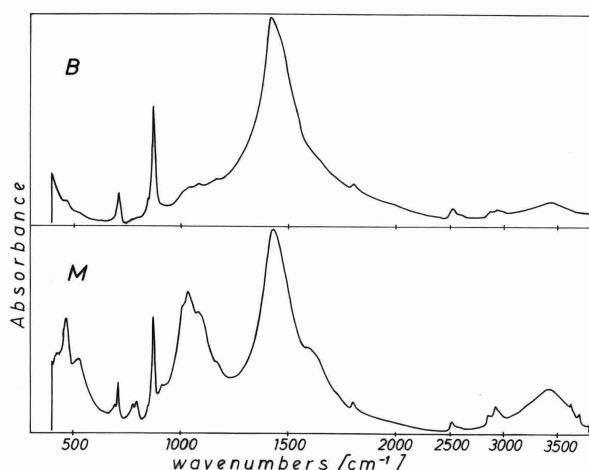
composed, we have performed infrared absorption measurements. It is known that IR spectroscopy is a powerful method for investigating minerals (anhydrous or hydrated carbonates, silicates, etc.) and phases with short-range atomic order. The spectra were measured for several pairs of samples. The result for section No. 7 ( $18^\circ C$ ) is presented in Figure 7. The differences for the loops B and M are evident, especially in the band centered at  $1050\text{ cm}^{-1}$  and in the region  $3000\text{--}4000\text{ cm}^{-1}$ . The spectra were analyzed based on references [17,18]. It appeared that the band at  $1050\text{ cm}^{-1}$  is connected with silica hydrosols and the intensity is much higher for the deposit M from treated water. Because silica hydrosols possess strong sorption properties, a remarkable difference in the range  $3000\text{--}4000\text{ cm}^{-1}$  coming from water molecule oscillations should be observed. One can see in Figure 6 that it does actually occur. The difference in calcite concentration is also visible here, as it was in the X-ray diffraction patterns (Fig. 6), chemical analysis (Tab. 1) and in PIXE measurements (Fig. 5). As far as the differences in concentration of metals (Fe, Mn, Cu, Zn, ...) are concerned, they are ascribed to the sorption properties of silica hydrosols.

**Table 1.** Proportional content of different elements in dry deposits from magnetically treated (M) and untreated (B) water, as determined by chemical analysis.

| Compound<br>/Section<br>number | SiO <sub>2</sub> | Fe <sub>2</sub> O <sub>3</sub> | CaO  | MgO  | SO <sub>3</sub> | Na <sub>2</sub> O | K <sub>2</sub> O | CuO  | Mn <sub>2</sub> O <sub>3</sub> | ZnO  | CO <sub>2</sub> | Total<br>% |
|--------------------------------|------------------|--------------------------------|------|------|-----------------|-------------------|------------------|------|--------------------------------|------|-----------------|------------|
| M – 13                         | 13.9             | 4.51                           | 37.7 | 1.6  | -               | 0.36              | 0.52             | 1.44 | 0.08                           | 0.74 | 36.9            | 97.75      |
| B – 13                         | 1.8              | 0.27                           | 48.6 | 5.1  | 5.1             | 0.25              | 0.13             | 0.20 | 0.01                           | 0.12 | 43.3            | 100.2      |
| M – 9                          | 18.5             | 3.15                           | 31.5 | 0.88 | -               | 0.28              | 0.65             | 2.73 | 0.08                           | 2.1  | 35.9            | 95.17      |
| B – 9                          | 4.9              | 0.88                           | 50.0 | 4.0  | 0.50            | 0.28              | 0.18             | 0.43 | 0.02                           | 0.23 | 40.1            | 99.8       |
| M – 7                          | 17.4             | 6.44                           | 29.6 | 2.57 | 0.42            | 0.31              | 0.64             | 1.29 | 0.07                           | 1.35 | 39.3            | 99.4       |
| B – 7                          | 10.5             | 1.65                           | 43.4 | 4.0  | 0.50            | 0.32              | 0.18             | 0.57 | 0.02                           | 0.28 | 38.5            | 99.8       |

**Table 2.** Result of chemical analysis of deposits recovered in three 200 MW blocks of the heat exchanger in Łaziska power plant from water treated with the MWT device. Relative contents of the elements is given.

|                 | Humidity<br>at 105 °C | Water<br>const. | CaO   | MgO   | Fe <sub>2</sub> O <sub>3</sub> | Mn <sub>3</sub> O <sub>4</sub> | ZnO  | Na <sub>2</sub> O | K <sub>2</sub> O | Al <sub>2</sub> O <sub>3</sub> | CO <sub>2</sub> | SiO <sub>2</sub> | SO <sub>3</sub> | P <sub>2</sub> O <sub>5</sub> | Total |
|-----------------|-----------------------|-----------------|-------|-------|--------------------------------|--------------------------------|------|-------------------|------------------|--------------------------------|-----------------|------------------|-----------------|-------------------------------|-------|
| Block<br>No. 9  | 19.66                 | 20.0            | 10.78 | 23.33 | 5.20                           | 0.20                           | 0.02 | 0.20              | 0.13             | 0.75                           | Not<br>disc.    | 19.30            | 0.76            | 1.39                          | 99.35 |
| Block<br>No. 10 | 18.0                  | 18.0            | 13.50 | 28.0  | 2.40                           | -                              | -    | -                 | -                | 0.60                           | -               | 24.0             | -               | 1.50                          | 98.0  |
| Block<br>No. 12 | 18.7                  | 20.0            | 30.96 | 4.68  | 1.23                           | 0.06                           | 0.25 | 0.21              | 0.10             | 0.56                           | Not<br>disc.    | 24.80            | 0.70            | 0.95                          | 99.40 |

**Fig. 7.** Infrared absorption spectra of deposits from B (untreated) and M (magnetically treated water) loops.

#### 4 Industrial application of MWT

Magnetic water treatment was put into practice in a number of industrial plants and, amongst the others, in the heat exchangers of the 1 GW electric power plant in Łaziska, Poland. A cooling system in the plant works in the half-closed cycle and uses water from coal-mines. Additional water for this system (*ca.* 5% of the whole volume) is subjected to the chemical process of decarbonization and coagulation and, as a result, water with lower carbonate hardness is obtained, however with increased and variable amount of suspensions of different origin. Chemical methods could not help the problem of carbonate sed-

iments, especially during hot summer periods when it was necessary to clean the system (mainly the heat exchangers working for turbine cooler) even every few weeks. Based on the positive results from the Pałnów experiment (see Fig. 3), it was decided to support the not fully effective chemical conditioning with the magnetic method.

Several new MWT devices [14] with the increased capacity of 1100 m<sup>3</sup>/h and with the enhanced hydrodynamics (see Fig. 2b) were installed at the inlet of the aid water. The results of the chemical analysis of the inlet water were following: Ca–107.4 mg/l, Mg–46.0 mg/l, Na–134 mg/l, K–17.4 mg/l, Fe–1.5 mg/l, SO<sub>4</sub><sup>2-</sup>–354 mg/l (7.38 mval/l), NO<sub>3</sub><sup>-</sup>–1.86/l (0.03 mval/l), Cl<sup>-</sup>–96 mg/l (2.7 mval/l), SiO<sub>2</sub>–12.3 mg/l, free CO<sub>2</sub>–22 mg/l (1 mval/l), pH = 8.0, carbonate hardness–5.3 mval/l, total hardness–9.14 mval/l, total suspended solids–17.4 mg/l, total solid residue–987 mg/l. Temperature of water was between 20 °C and 35 °C. Deposits were investigated for three 200 MW blocks. The result of using the MWT was amazing. It appeared that all the three sections of the cooling system did not become encrusted with scale and several months after the start, only a small amount of soft and loose deposit has been recovered from the curved parts of the tubes. The chemical analysis of the deposit was performed in a plant laboratory. Next, the physical measurements (X-ray diffraction, IR, PIXE, DTA, SEM and the measurement of a specific surface area) were carried out.

Table 2 presents result of chemical analysis of deposits. The amount of CO<sub>2</sub>, usually observed in the deposits in that plant was 30%–40%. On the contrary, the CO<sub>2</sub> content in the MWT deposit determined with the routine procedure was practically equal zero. The analyses definitely showed that the deposits were not limescale carbonates.

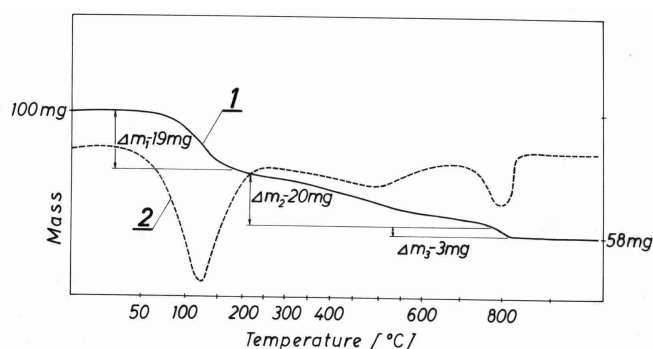


**Fig. 8.** DTA result for the deposit from the magnetically treated water: full line - mass of the sample as a function of temperature, for description of  $\Delta m_1$ ,  $\Delta m_2$  and  $\Delta m_3$ , see text; dotted line - temperature mass derivative.

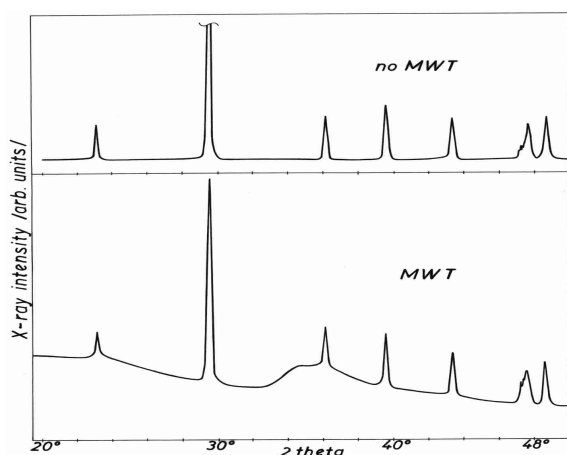


**Fig. 9.** X-ray diffraction patterns for deposits recovered in the industrial cooler with the MWT device (lower curve) and without MWT (upper curve).

Another interesting result was a high humidity, 19% on average and about 20% water of crystallization in the dried samples of deposits from three blocks. In comparison with Table 1 there was more Si and Mg. The results for three cooling blocks were similar.

In order to check the water and  $\text{CO}_2$  content by another method, the thermogravimetric analysis (DTA) for the MWT deposit from Block 10 was performed using a Mötler apparatus. Curve 1 in Figure 8 shows mass of the sample as a function of temperature. The loss of water (humidity) taking place up to 140 °C gave the mass change  $\Delta m_1 \approx 19\%$ , the loss of water of crystallization occurring up to 750 °C gave  $\Delta m_2 \approx 20\%$  and the loss of  $\text{CO}_2$  in the range 750 °C–800 °C gave  $\Delta m_3 \approx 3\%$ . Curve 2 shows the derivative of mass change. Thus, the lack of carbonates in the deposit was confirmed. The small amount of  $\text{CO}_2$  observed by DTA was probably due to carbonates crystallized before the entrance to the block.

One pair of X-ray diffraction patterns for the deposits without and with MWT is given in Figure 9. The MWT spectrum was obtained with the high X-ray detector am-

plification. The unconditioned water showed a low background and strong peaks of a crystalline phase, identified as the Mg-substituted calcite. The main part of the sample obtained from conditioned water were the amorphous substances with only short range atomic order, as followed from the high background and two broad humps present in the pattern. Reflections coming from calcite gave about 5% of total intensity.

Figure 10a presents the IR spectra obtained with “Digilab” spectrometer with Fourier analysis. Curve 1 is for pure calcite. Curve 2 is a typical spectrum for deposits from the magnetically treated water. Like spectrum M in Figure 7, it shows the remarkable enhancement of the  $1050\text{ cm}^{-1}$  band coming from silica hydrosol, and, on the other hand, suppression of the calcite bands. Curve 3 shows the absorbance for the MWT deposit after treating with a 5% solution of HCl (the same result was obtained with the 1-molar acetate acid). The main features of the spectrum obtained are identical to those of a common silica gel, the IR spectrum of which is given in Figure 10b. This confirms the presumption that it is silica, which is responsible for the effects observed for MWT. Little of the strong calcite peak at  $850\text{ cm}^{-1}$  is seen in spectrum 2 and the one at  $1500\text{ cm}^{-1}$  has about 5% of intensity it has the spectrum 2. Vibrations of the absorbed water in the range  $3200\text{--}3600\text{ cm}^{-1}$  are about 4 times weaker in calcite than in the curve 2, which is due to high water concentration in MWT deposits. The peak at  $3700\text{ cm}^{-1}$  comes from brucite. The changes obtained after treating the MWT deposit with 5% HCl are following: the band at  $1550\text{ cm}^{-1}$  coming from calcite has disappeared, the same happened to the  $3700\text{ cm}^{-1}$  brucite line. The bands at  $1000$  and  $1100\text{ cm}^{-1}$  curve 2 have been shifted to about  $1100\text{ cm}^{-1}$  and  $1200\text{ cm}^{-1}$ , what is probably connected with polymerization of silica hydrosols.

The specific surface area determined for MWT deposits was  $80\text{ m}^2/\text{g}$ . This is the very high value, especially for the material, which had already worked as an adsorbent. Such a highly developed surface is typical for silica gel and supports the conclusion about the crucial role of silica in the MWT effect. Coming back to Table 2 one should notice the remarkable sorption efficiency of the magnetically activated silica: 23% (in average) of silica adsorbs *ca.* 18% of calcium or magnesium.

Figure 11 compares SEM photos of the substances investigated. Crystallites of pure  $\text{CaCO}_3$  are shown on the left, in the middle – the example of an open-work sphere of  $\text{CaCO}_3 \cdot \text{H}_2\text{O}$ . Spheres, such as that, or closed-packed spherulites were obtained by us when performing laboratory studies of the crystallization kinetics of carbonates. They used to crystallize in water with a high concentration of magnesium [20]. The effect of magnesium ion on crystallization of  $\text{CaCO}_3$  polymorphs has been recently investigated also in [21]. The SEM photo on the right of Figure 11 shows an example of the amorphous deposit formed in the heat exchanger with magnetically treated water. A large number of photos were taken for MWT deposits; all were similar.

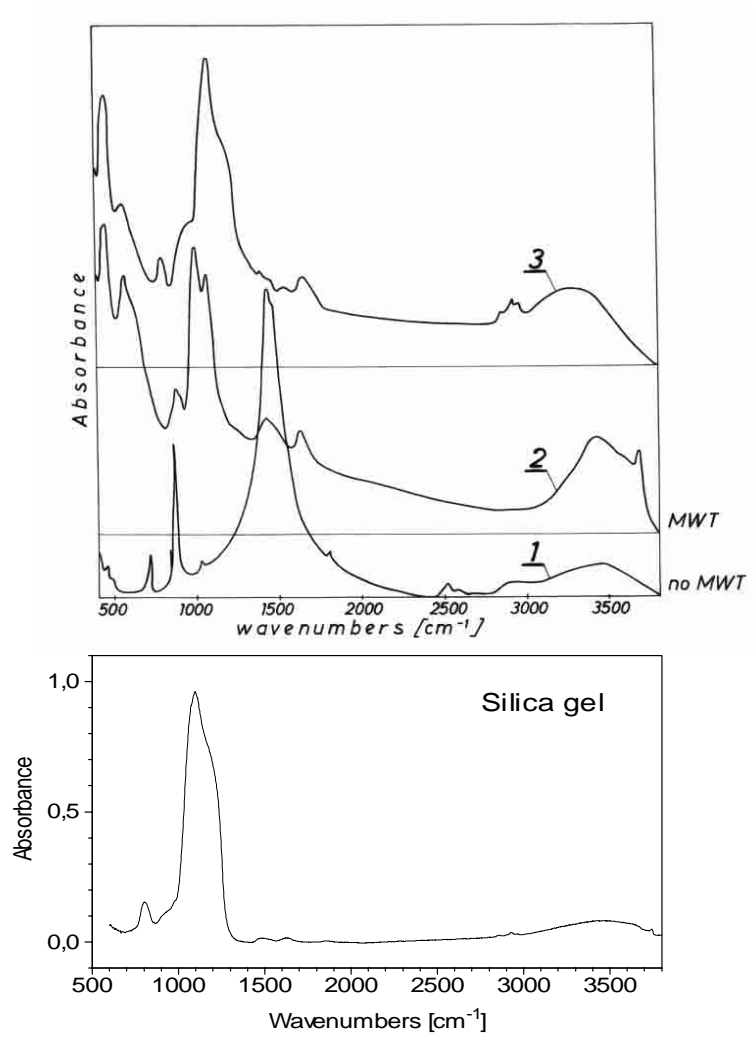


**Fig. 10.** Infrared absorption spectra: (a) (1) normal scale with the main component of calcite; (2) deposit recovered after MWT - main contribution from Ca-Mg-silicasols; (3) as in (2) but after scouring with 5% solution of HCl; (b) spectrum of the industrially produced silica gel.

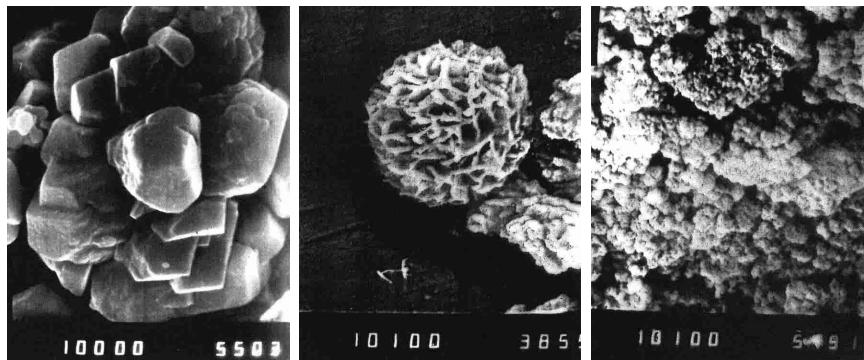


**Fig. 11.** SEM photos: left - pure calcite; middle - monohydrocalcite in the form of open-work spherulite; right - amorphous Ca-Mg-silica hydrogel, MWT deposit (see text).

## 5 Discussion

Results obtained from the large-scale experiment and from industrial practice show that magnetic water treatment does work on an industrial scale. We did not observe scaling of surfaces of heat exchangers but a small amount of soft, amorphous deposit. Infrared absorption spectra allowed identification of that deposit, as coming from a silica hydrosol and this finding is the main result of our study. One should note that the characteristic line at  $1100\text{ cm}^{-1}$  belonging to silica hydrosol appears also in the Fourier transform infrared spectrum of the precipitate obtained after the electromagnetic water treatment [22].

The fact that silica was responsible for a spectacular anti-scale effect of the magnetic treatment of natural water is undoubtedly of importance. Silica is the most abundant natural material and can occur in a number of forms [23]. Industrially produced active silica (technical nomenclature) which is a colloidal silica hydrosol, is an important flocculant, used for supporting coagulation processes. Active silica has a short validity period and should be preferably used during 2–3 days [24]. That period coincides amazingly with the observed in literature [2, 10–13, 15] duration of the MWT effect. A popular silica gel is a strong adsorbent. We suppose that in MWT crystallization of calcite is blocked just due to adsorption of calcium, magnesium or other metal ions by the “magnetically activated” silica. In the course of the further discussion we will try to explain what is meant under that term.

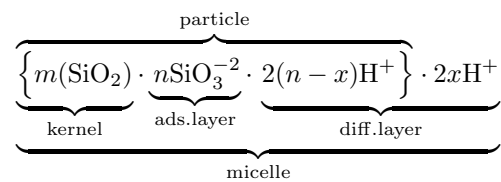
As it was mentioned in Introduction, natural water should be concerned as a dilute colloidal solution. Phenomena occurring in colloidal water solution are difficult to describe due to their complexity and dependence on a number of physical and chemical parameters. It is known that colloidal systems are characterized by electrostatic charges of their particles, relative to the solvent. The electric double layer at a solid-liquid interface determines electrokinetic properties of the system. Stability or coagulation of the colloid depends on electrostatic repulsion versus intermolecular attraction forces. External electric field or Lorentz forces in a magnetic field (as in MWT) will influence the system behavior. Since the first theoretical approach by Smoluchowski [25], kinetics of coagulation and electrochemistry of colloidal solutions has been the subject of intensive research. Two papers [16, 26] based on the recognized DLVO (Derjaguin, Landau, Verwey, Overbeek) theory [27] discuss the processes occurring or initiated in natural water passed through the magnetic device. In the paper on the action of a static magnetic field on moving solutions and suspensions [26] Gamayunov considers a Lorentz force induced change (deformation) of the electric double layer. This deformation leads to a temporary decrease of repulsion barrier and hence to an increased coagulation tendency of disperse particles. The conception above allowed the author to explain a magnetic field effect on coagulation and sedimentation in chalk suspensions. The recent paper by Lipus *et al.* [16] presents a developed model of surface neutralization as one of the possible mechanisms of scale control by MWT. Neutralization can occur due to shifts of ions from the bulk of the

solution toward the particle surface. The ion shift by the Lorentz force is balanced by the viscosity force. According to [16], the Lorentz shift of an ion is given

$$\Delta x = \frac{e}{6\pi\eta r} \frac{z}{r} B\tau\nu,$$

where  $e$ -electron charge,  $z$ -ion valence,  $\eta$ -water viscosity,  $r$ -ion radius,  $B$ -magnetic field density,  $\tau$ -retention time in MWT device and  $\nu$ -flow velocity. The shifts estimated at  $B\nu = 0.2\text{ V/m}$  and  $\tau = 0.1\text{ s}$  are equal to 3.4 nm and 5.3 nm for  $\text{Ca}^{2+}$  and  $\text{Mg}^{2+}$ , respectively, while for  $\text{HCO}_3^-$  one gets 0.9 nm. Ions shifts become essential in the vicinity of solid surfaces, where they could cause condensation of the Stern adsorption layer on account of the diffuse layer. The authors claim that shifted counterions will remain adsorbed in the Stern layer for a longer time (even for days) depending on the degree of neutralization. (It was actually found by AFM in [12] that magnetic exposure thickened the adsorbed layer; the fact was explained as coming from the adsorption of hydrated ions.) Finely, the conclusion is made that antiscaling effect is possibly caused by accelerated coagulation of scale-forming particles during and after MWT.

We think that the models cited above give a good support for our conclusion about the crucial role which is played by silica. Although the two cited papers were discussing Lorentz force effects on any colloidal particle, the role of silica is somehow unique. Silica is present in natural water in the form of silicic acid polymers  $x\text{SiO}_2 \cdot y\text{H}_2\text{O}$ , which can easily evolve into the ionic or colloidal state, and in the form of colloidal particles  $(\text{SiO}_2)_m$  of a diameter up to  $1\ \mu$ . Silica's content in water ranges from 1 mg/l (or less) up to 10 mg/l (or more). In the stable colloidal solution silica particles are neutralized (non-active) and form micelles [24] of the schematic structure:



Silica colloidal particles are strongly negatively charged (18, 22–24) due to  $\text{SiO}_3^{2-}$  anions coming from the dissociation of the kernel surface. Negative charge remains unchanged in the wide range of pH and this is the property which differentiates silica particles from other, easily rechargeable, colloidal particles. An extensive diffuse layer (diff. layer) consists of  $\text{H}^+$  ions and of other positive ions present in the solution (*e.g.*  $\text{Ca}^{2+}$ ,  $\text{Mg}^{2+}$ , ...). In the diffuse layer also  $\text{H}_2\text{O}$  molecules are present. They can be somehow oriented [28].

The negative charge revealed by the action of Lorentz force should facilitate adsorption of positively charged ions or particles. The shift of ions caused by the Lorentz force from the diffuse layer into the Stern layer will be the most pronounced for Ca- and Mg-cations, due to their small  $r/z$  ratio. According to [16], the relative shift (*i.e.* related to the length of the diffuse layer) estimated for  $\text{Ca}^{2+}$  and

Mg<sup>2+</sup> ions in the domestic tap water would be 1.9 and 3, respectively, in the MWT device of the  $B\nu\tau$  product four times less than of our device (see Chap. 2). Shifted cations would remain adsorbed at the negatively charged surface of the colloidal particle for a longer time [16]. This process is probably strong enough to block crystallization of Ca- and Mg- carbonates. Thus, by magnetic activation we mean a field induced modification of the diffuse layer which promotes adsorption of cations by colloidal particles. Our results show that this process is especially important for colloidal silica. The other change, which can here occur, is the enhanced possibility of coagulation of the dispersed system. We are aware that the silica sol and the silica-water interface present the very complex systems [29], which should be studied with great caution. Undoubtedly, a further experimental work is desirable for quantitative description of MWT antiscaling effect.

Finally, let us compare the average amounts of suspension and deposits recovered in our large-scale experiment. Mass of water flowing through each loop was 2500 t. The average dry mass remaining after vaporization of 1 liter of water used was 0.35 g. This gives more than 800 kg of suspension, which flowed through every loop during four months. The silica content in water was 10 mg/l, which gave 25 kg of silica. Formation of carbonate deposits at moderate temperatures (up to 30 °C) was a slow process, as only 190 g in total of calcite deposit was recovered in loop B after four months. It is seen that to prevent the system against limescale it was necessary to activate only a small fraction of silica present in water.

In summary, we have presented results of a large-scale experiment and an industrial application of magnetohydrodynamic water treatment. Thanks to the long duration and proper realization of the treatment the spectacular antiscaling effect was obtained. Amorphous, soft deposit recovered with MWT was identified as coming from silica hydrosol. It appeared that crystallization of calcite was blocked due to strong adsorption of calcium and other metal ions on magnetically activated silica. As a result, amorphous Ca-Mg-silica hydrosols were created in processes of adsorption and coagulation. We suppose that colloidal silica was activated through a Lorentz force induced condensation of Stern layer on account of diffuse layer [16]. In order to prevent the system against limescale it was necessary to activate only a small fraction of present in water silica.

We would like to express our sincere thanks to the team of "Energopomiar" Chemical Department in Gliwice, Poland for performing chemical analyses and for the fruitful cooperation. The help and kind attitude of the director and technical staff of the Łaziska power plant is also deeply acknowledged. We are very grateful to our colleagues, J. Ściesiński and A. Bajorek for the measurements of the IR absorption and X-ray diffraction patterns. Additional measurements and discussions of results with groups of Professor M. Handke and Professor S. Hodorowicz are kindly acknowledged. Special thanks we are due to Professor J.M.D. Coey for the help with the text and the discussion.

## References

1. Th. Vermeiren, *Corrosion Technol.* **5**, 215 (1958).
2. V.I. Klassen, *Dokl. Akad. Nauk SU* **166**, 1383 (1966); *Omagnicivanije vodnych sistem (in Russian)* (Ed. Chimija, Moskva, 1978); in *Developments in Mineral Processing* (Elsevier, N.Y., 1981), Part B, Mineral Processing, p. 1077.
3. K.J. Kronenberg, *IEEE Trans. Magn.* **21**, 2059 (1985).
4. E.F. Tebenihin, B.T. Gusev, *Obrabotka vody magnitnym polem v teploenergetike* (Ed. Energija, 1970).
5. N.N. Kruglitskij, G.A. Kataev, B.P. Zhantalay, K.A. Rubezhanskij, A.A. Kolomec, *Kolloid. Zh.* **47**, 493 (1985).
6. S.A. Parsons, B.L. Wang, S. Udol, S.J. Judd, T. Stephenson, *Trans. IChemE (part B)* **74**, 98 (1997).
7. I.J. Lin, J. Yotvat, *J. Magn. Mater.* **83**, 525 (1990).
8. V.G. Levic, *Uspekhi Fiz. Nauk* **88**, 787 (1966) (in Russian).
9. O.T. Krylov, I.K. Vikulova, V.V. Eletsy, N.A. Rozno, V.I. Klassen, *Coll. J. USSR* **47**, 31 (1985).
10. K. Higashitani, K. Okuhara, S. Hatade, *J. Colloid Interface Sci.* **152**, 125 (1992).
11. K. Higashitani, H. Iseri, K. Okuhara, A. Kage, S. Hatade, *J. Colloid Interface Sci.* **172**, 383 (1995).
12. K. Higashitani, J. Oshitani, *J. Colloid Interface Sci.* **204**, 363 (1998).
13. J. Oshitani, R. Uehara, K. Higashitani, *J. Colloid Interface Sci.* **209**, 374 (1999).
14. *Anti-scale Magnetic Treatment and Physical Conditioning, Proc. MAG 3 (Ed. S. Parsons, Cranfield University, 1999)*, ISBN - 1 86194 010 6.
15. J.M.D. Coey, S. Cass, *J. Magn. Mater.* **209**, 71 (2000).
16. L.C. Lipus, J. Krope, L. Crepinsek, *J. Colloid Interface Sci.* **236**, 60 (2001).
17. V.C. Farmer, *The Infrared Spectra of Minerals* (Mineralogical Society Monograph 4, London, 1974).
18. W. Eitel, *The Physical Chemistry of the Silicates* (The University of Chicago Press, 1954).
19. A. Szkatuła *et al.*, Magnetohydrodynamic method of water treatment, European Patent No. 0241 090 B1, Cl. C02F 1/48.
20. A. Szkatuła *et al.*, in preparation.
21. M. Kitamura, *J. Colloid Interface Sci.* **236**, 318 (2001).
22. M. Colic, D. Morse, *Langumir* **14**, 783 (1998).
23. R.K. Iler, *The Chemistry of Silica* (Wiley, New York, 1979).
24. L.A. Kulskii, *Theoretical Bases and Technology of Water Conditioning* (Ed. Naukova Dumka, Kiev, 1980) (in Russian).
25. M. Smoluchowski, *Phys. Zeit.* **XVII**, 557–571; 587–599 (1916).
26. N.I. Gamayunov, *Kolloid. Zh.* **56**, 290 (1994); English Translation: *Colloid. J.* **56**, 234 (1994).
27. R.J. Hunter, *Introduction to Modern Colloidal Science* (Oxford Science Publications, New York, 1996).
28. Q. Du, E. Freysz, Y.R. Shen, *Phys. Rev. Lett.* **72**, 238 (1994).
29. V.V. Yaminsky, B.W. Ninham, R.M. Pashley, *Langumir* **14**, 3223 (1998).